

Supporting Information

Chemically Induced Proximity System Engineered from the Plant Auxin Signaling Pathway

Weiye Zhao, Huong Nguyen, Guihua Zeng, Dan Gao, Hao Yan and Fu-Sen Liang*

Department of Chemistry and Chemical Biology, University of New Mexico, 300 Terrace Street
NE, Albuquerque, New Mexico 87131, United States

*Corresponding Author: fsliang@unm.edu

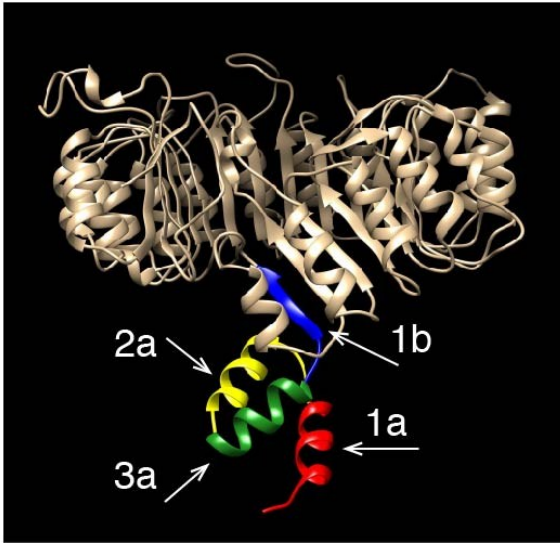
Table of Contents

Figure S1-S11.....	3
Experiment details.....	14

Oryza sativa TIR1 7 10
MTYFPEE**EV**EHIFSFLPAQR
Arabidopsis thaliana TIR1 MXSFPE**EV**LEHVFSFIQLDK
 12 15

Figure S1. The sequence alignment of the region on TIR1 proteins engaged in TIR1-SCF complex binding. Alignment was performed using Phyre2.

(a)



(b)

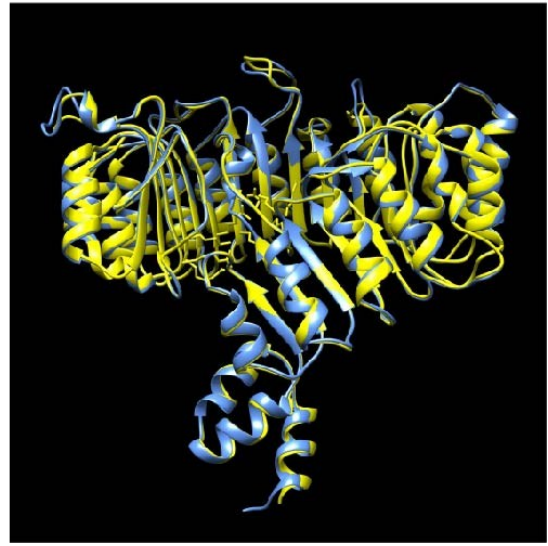


Figure S2. Modeled three-dimensional structure of *Oryza sativa* TIR1 (osTIR1) by Phyre2 protein fold recognition program. (a) Predicted structures of osTIR1. (b) Superimposed structure of osTIR1(blue) and *Arabidopsis* TIR1(yellow).

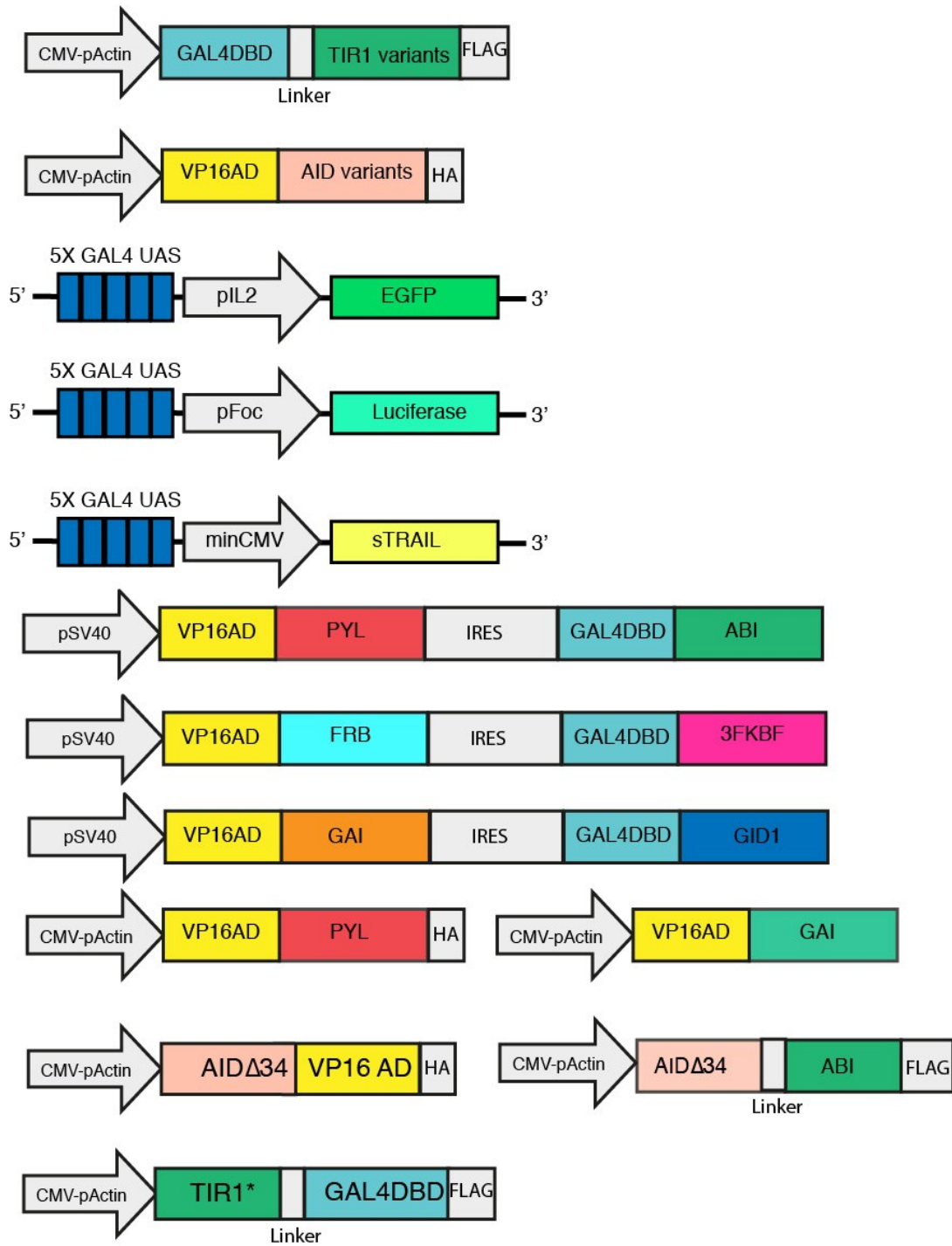


Figure S3. Constructed plasmids described in this work. (TIR1 variants include wild type TIR1, TIR1*, TIR1**, TIR1-1a, TIR1-2a, TIR1-3a and TIR1-4b. AID variants include wild type AID, AID Δ 34 and AID Δ 134.)

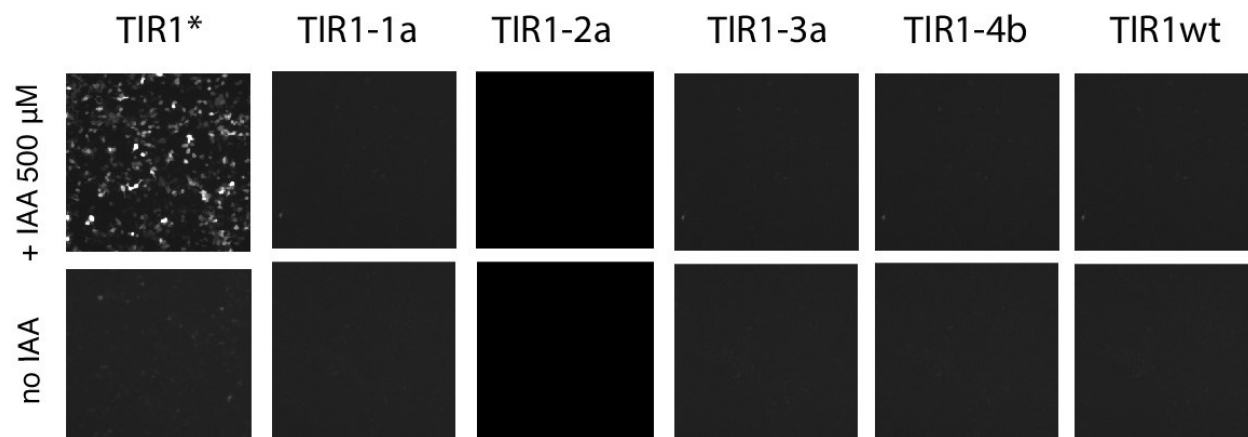


Figure S4. EGFP expression induced by IAA (500 μ M) using GAL4DBD-fusion proteins containing different versions of osTIR1s.

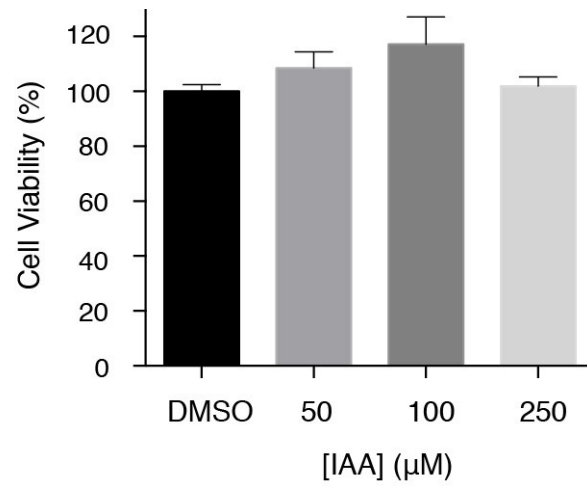


Figure S5. Analysis of the cytotoxicity of IAA by the MTT assay in CHO cells. The percentages of cell viability were calculated by comparing IAA-treated cells to DMSO-treated ones. Error bars represent \pm s.e.m. from replicates ($n = 6$).

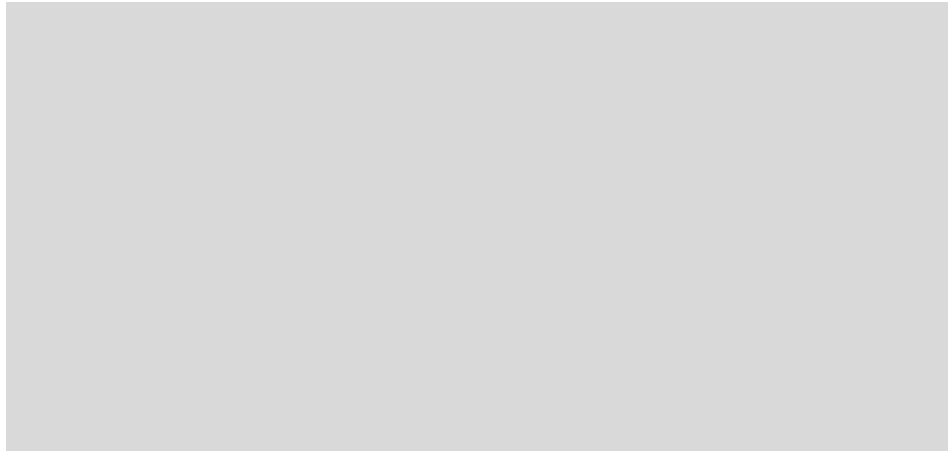


Figure S6. Sequence alignment of two critical regions of TIR1s impacting TIR1-AID binding. Alignment was performed using Phyre2.

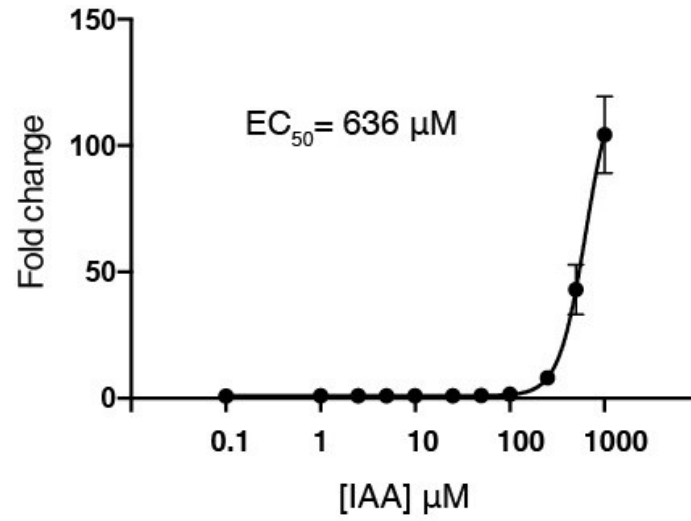


Figure S7. Dosage response of IAA-induced luciferase expression using GAL4DBD-TIR1** and VP16AD-AIDΔ34 plasmids for 24 h. Fold changes of induced luciferase expression were calculated based on DMSO treated samples. Error bars represent \pm s.e.m. from independent cell assays ($n = 3$).

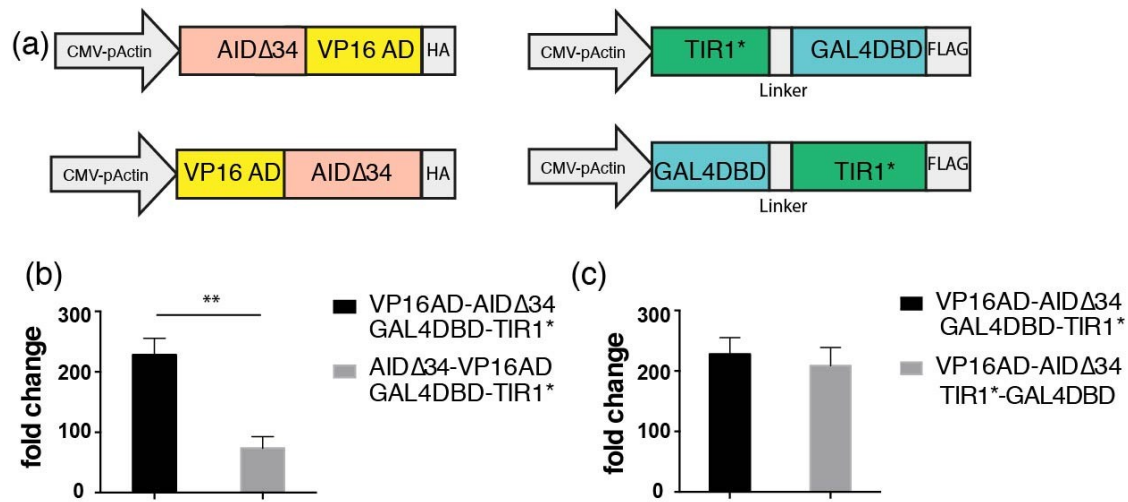


Figure S8. Effects of the positions that POIs were fused to TIR1* or AID Δ 34. (a) Constructs of tested fusion proteins. (b) IAA-induced luciferase expression using fusion proteins with VP16AD fused to either N or C-terminus of AID Δ 34. (c) IAA-induced luciferase expression using fusion proteins with GAL4DBD fused to either N or C-terminus of TIR1*. Fold changes of induced luciferase expression were calculated based on DMSO treated samples. Error bars represent \pm s.e.m. from independent cell assays (n = 3).

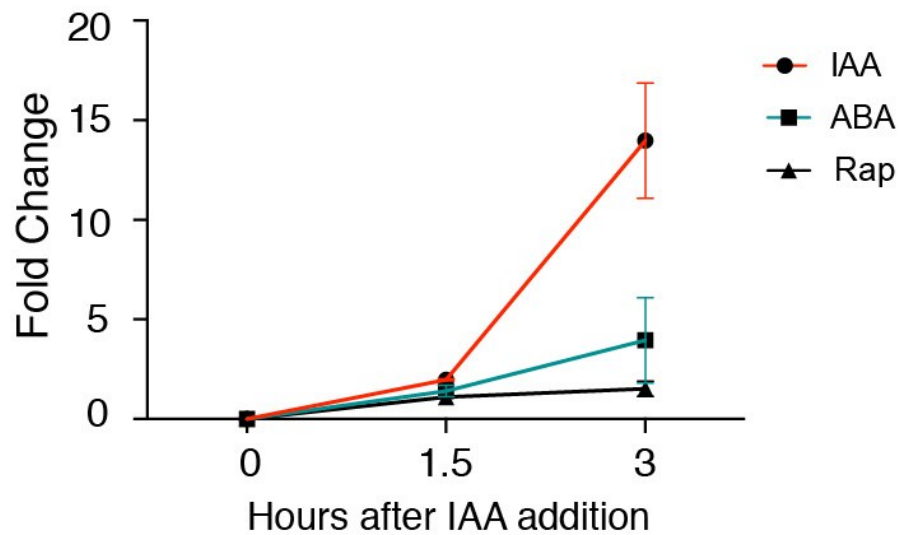


Figure S9. The early time courses of IAA- (250 μ M), ABA- (50 μ M), and Rap (10 nM) induced luciferase expression. CHO cells were transfected with individual split transcriptional activator constructs and treated with corresponding inducers for indicated time periods. Luciferase activities were then quantified. Fold changes of induced luciferase expression were calculated based on DMSO treated samples. Error bars represent \pm s.e.m. from independent cell assays (1.5 h, n = 3; 3 h, n= 2).

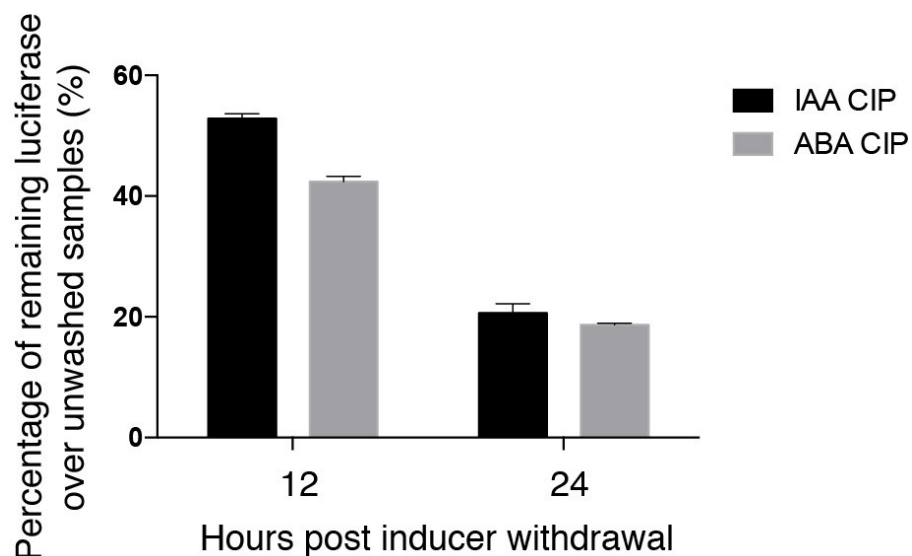


Figure S10. Remaining luciferase activity upon inducer withdrawal. Transfected CHO cells were treated with IAA (250 μ M) or ABA (100 μ M) for 24 h and then washed with fresh cell culture media without IAA or ABA for three times to remove inducers (or not washed as a control). Luciferase activities were then quantified. Percentages were calculated by comparing the luciferase activity under each washing condition to the corresponding unwashed sample. Error bars represent \pm s.e.m. from independent cell assays (n = 3).

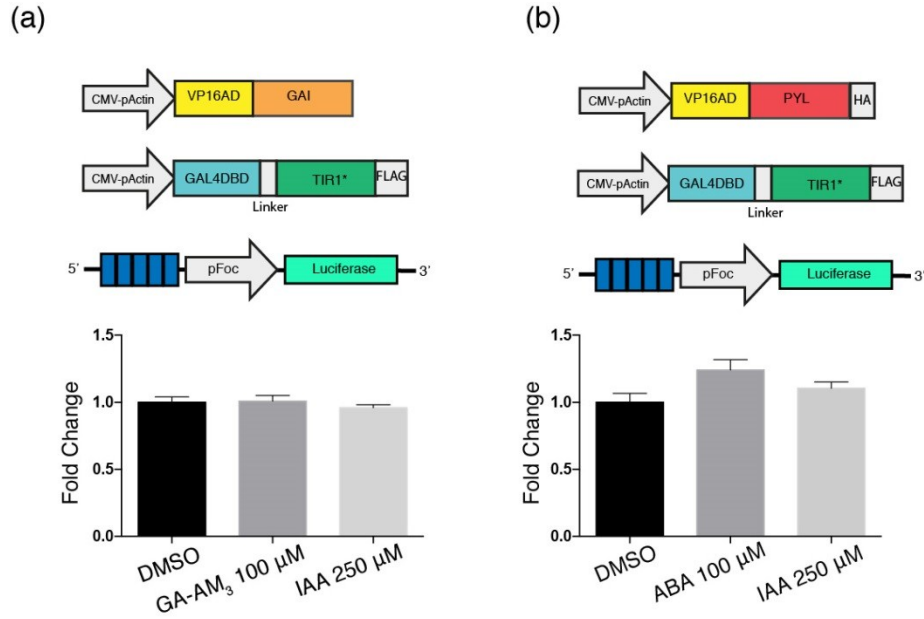


Figure S11. Orthogonality of IAA and GA-based CIP systems. Transfected with mismatched dimerizing protein pairs (VP16AD-GAI and GAL4DBD-TIR1*, or VP16AD-PYL and GAL4DBD-TIR1*), CHO cells were treated with small-molecule inducers for 24 hours, and subjected to luciferase assay. Fold changes of induced luciferase expression were calculated based on DMSO treated samples. Error bars represent \pm s.e.m. from replicates ($n = 4$).

Experiment details

Reagents and DNA plasmids construction.

IAA was purchased from Sigma (Cat# I3750). ABA was purchased from Gold Biotechnology (Cat# A-050-5). Polyethylenimine (PEI, Polysciences) was employed as transfection reagent. All DNA fragments were amplified by polymerase chain reaction (PCR) using either Q5 DNA polymerase (New England Biolabs) or CloneAmp HiFi PCR Premix (Clontech) under S1000 thermal cycler with Dual 48/48 Fast Reaction Module (Bio-Rad). All restriction enzymes are commercially available from New England Biolabs. All TIR1 variant DNA fragments were amplified by using pBabe TIR1-9myc (Addgene #47328) as template. To clone all pActin-GAL4DBD-TIR1 variants constructs, we replaced the GFP fragment pActin-GFP-PYL construct by GAL4DBD fragment using Sall and AscI cutting sites, and inserted each of the TIR1 variants into pActin-GFP-PYL¹ construct which was linearized by AscI and NotI restriction enzymes, while the AscI restriction cutting site was replaced by MluI through In-Fusion DNA recombination process. We shifted the order of TIR1* and GAL4DBD fragments to construct pActin-TIR1*-GAL4DBD. For this, we cloned TIR1* and GAL4DBD into pActin-GAL4DBD-TIR1* by Sall, MluI and MluI, NotI restriction sites, respectively. All AID variant DNA fragments were amplified by using pcDNA5-H2B-AID-EYFP construct (Addgene #47329) as template. For all pActin-VP16AD-AID variants constructs, VP16AD (by Sall and AscI restriction cutting sites) and each of the AID variant (by AscI and NotI restriction cutting sites) were cloned into pActin-GFP-PYL accordingly. Actin-AID Δ AID34-VP16AD was obtained by altering the order of VP16AD and Δ AID34 fragments of Actin-VP16AD- Δ AID34. Δ AID34 was inserted by using Sall and AscI sites and VP16AD was cloned in by AscI and NotI cutting sites, respectively. pSV40-VP16AD-GID1-IRES-GAL4DBD-GAI was obtained by substituting GID1 and GAI fragments for PYL and ABI fragments in pSV40-VP16AD-PYL-IRES-GAL4DBD-ABI construct, respectively. pActin-VP16AD-PYL-HA and pActin-VP16AD-GAI were derivative from pSV40-VP16AD-PYL-IRES-GAL4DBD-ABI and pSV40-VP16AD-PYL-IRES-GAL4DBD-ABI by using BamH1 and Not1, respectively, and the SV40 promoter was substituted by Actin promoter. pActin-AID Δ 34-ABI was obtained by cloning AID Δ 34 into pActin-GAI-ABI² through Sall and MluI. An inducible plasmid vector expressing secretable TRAIL was made by inserting the nucleotide sequence corresponding to i) the N terminal secretion signal sequence of human IL-2R α (MDSYLLMWGLLTFIMVPGCQA) and ii) the C terminal extracellular domain of human TRAIL (aa 114-281) downstream of the minimal CMV gene promoter and five copies of Gal4 DNA binding sites (CGGAGTACTGTCCCTCCGAG). Primers designed for cloning the constructs used in this study are listed below:

VP16AD (F): 5'- CCGACAGTCGACGCCACCATGGGCCCTAAAAAGAAGCGT
 VP16AD (R): 5'- CCGACAGGCGCGCCCCACCGTACTCGTCAATTCC
 GAL4DBD (F): 5'- CCGACAGTCGACGCCACCATGAAGCTACTGTCTTCTATC
 GAL4DBD (R): 5'-
 CCGACAACGCGTAGATCCTCCTCCAGATCCCCACCCGATACAGTCAACTGTCTTTG
 TIR1 (F): 5'- TCTGGAGGAGGATCTACGCGTATGACGTA CT TCCCGGAGGAG
 TIR1* (F): 5'-
 TCTGGAGGAGGATCTACGCGTATGACGTA CT TCCCGGAGAAGGTGGTGAAGCACAT
 CTCA
 TIR1-1a (F): 5'- TCTGGAGGAGGATCTACGCGTCTGCCGGCGCAGCGCGACCGC
 TIR1-2a (F): 5'- TCTGGAGGAGGATCTACGCGTGTCTGCAAGGTGTGGTACGAG
 TIR1-3a (F): 5'- TCTGGAGGAGGATCTACGCGTCGCCGCGGCGTCTTCGTGGGC
 TIR1-4b (F): 5'- TCTGGAGGAGGATCTACGCGTGGCAACTGCTACGCCGTGCGC
 TIR1-FLAG (R): 5'-
 TTATGATCTAGAGTCGCGGCCGCTCTACTTGTTCGTCATCGTCTTTGTAGTCTAGGATT
 TTAACAAAATTTGG
 AID (F): 5'- CCGACAGGCGCGCCAATGATGGGCAGTGTCGAGCTG
 AID^Δ 134 (F): 5'- CCGACAGGCGCGCCAAGAGAGGGTTCTCAGAGACG
 AID-HA (R): 5'- CCGACAGCGGCCGCCTAAGCGTAATCTGGAACATCGTATGGGTA
 AGCTCTGCTCTTGC ACTTCTC
 AID^Δ34-HA (R): 5'-
 CCGACAGCGGCCGCCTAAGCGTAATCTGGAACATCGTATGGGTAAGCTCTGCTCTTG
 CACTTCTC
 ΔAID_{-ABI} (F): 5'- CCGACAGTCGACGCCACCATGATGGGCAGTGTCGAGCTGAAT
 ΔAID_{-GSGGGGSG} (R):
 CCGACAACGCGTACCTGATCCACCTCCACCAGATCCGTTCTTCCGGTATGATCTCAC

Cell culture and transfection.

Chinese hamster ovary (CHO) cell, human embryonic kidney HEK293T cell and MDA-MB-231 cell were cultured in Dulbecco's modified Eagle's medium (DMEM) (Gibco) supplemented with 10% FBS (Atlanta Biologicals) and GlutaMax (Gibco) in the humid atmosphere containing 5% CO₂. Cells were plated into 24-well plates one day prior to transfection. Cell culture medium was changed to fresh ones 4 h after the addition of transfection reagents. For transfection of cells in each well of 24-well plate, 400-500 ng of CIP plasmids and 125 ng reporter plasmid, along with

1.575-1.8 μg PEI, were mixed with 50 μL Opti-MEM (Gibco) and incubate at room temperature for 20 min. 50 μL of the transfection reagent were added to each of the wells.

Luciferase assay.

Luciferase assay was performed as described in our previous publication.¹ Briefly, cells were transfected with luciferase reporter gene and plasmids encoding variant CIP proteins. Small-molecule inducers at desired concentrations were added to the cultured cells 24 h after transfection. Cells were then harvested and lysed at the proper time points after small-molecule treatment. Then, signals were detected by GloMax-Multi Detection System (Promega) upon the addition of luciferase reagent.

MTT assay.

CHO cells were plated into 96-well plate and were cultured overnight. Cells were treated with IAA at different concentrations, as well as DMSO mock. Cells were subjected MTT assay 24 hours after IAA treatment, which was conducted as described in our previous publication.³

Fluorescence microscopy.

The fluorescence imaging was conducted by Zeiss Axio Observer D1 outfitted with HBO 100 microscopy illumination system. EGFP was excited at 470/40 nm and emitted fluorescence at 525/50 nm. Images were taken with GFP channel accordingly.

Cytotoxicity assay and quantification of secreted TRAIL.

For sTRAIL apoptotic assays, 293T cells were transfected to express the IAA-responsive split transcriptional activator and 5xGal4 response elements controlling the expression of sTRAIL. Cell culture supernatant containing sTRAIL was collected after 24 h treated with either IAA 250 μM or mock DMSO and incubated with TRAIL-sensitive MDA-MD-231 cancer cell lines for another 24 h. Cell viability and apoptosis were accessed using the Dead Cell Apoptosis Kit with Annexin V-FITC and PI, for flow cytometry according to the manufacturer's protocol (Invitrogen #V13242). Briefly, cancer cells were harvested by trypsinization at 24 h after drug treatment and were washed twice with cold PBS. Then 10⁶ cells, suspended in Annexin V binding buffer, were incubated with Propidium Iodide and FITC-Annexin V to a final concentration of 1 $\mu\text{g}/\text{mL}$, 1:20 volume ratio, respectively, for 15 minutes at room temperature in

the dark. Following which, 400 μ L Annexin-Binding Buffer was added and the stained cells were immediately analyzed by flow cytometry (BD Accuri™ C6 cytometer).

The concentration of secreted TRAIL in the supernatant was determined via human TRAIL PicoKine™ ELISA kit (Boster Biological Technology) according to the user manual.

Statistical analysis.

Data are expressed as mean values \pm s.e.m. Student's t-test statistical analyses were performed using GraphPad Prism 6.0 software when applicable. The dosage response curve was generated by nonlinear regression and the EC₅₀ was calculated accordingly using GraphPad Prism 6.0 software.

Structure prediction and sequence alignment.

The three-dimensional structure of osTIR1 was modeled through Phyre2 protein fold recognition program.⁴ The amino acid sequence of osTIR1 was loaded into Phyre2 online portal and the prediction was conducted by the program with the known Arabidopsis TIR1 structure (PDB: 2P1M)⁵ as template. Three-dimensional structures were visualized by UCSF Chimera software. Homologous alignment was performed by Phyre2. Query sequence and template sequence were aligned under the default settings of these online portals.

Reference

1. G. Zeng, R. Zhang, W. Xuan, W. Wang and F. S. Liang, *ACS Chem Biol*, 2015, 10, 1404-1410.
2. G. Zeng, H. Li, Y. Wei, W. Xuan, R. Zhang, L. E. Breden, W. Wang and F. S. Liang, *ACS Synth. Biol.*, 2017, 6, 921-927.
3. H. Yan, U. Bhattarai, Z.-F. Guo and F.-S. Liang, *J. Am. Chem. Soc.*, 2017, 139, 4987-4990.
4. L. A. Kelley, S. Mezulis, C. M. Yates, M. N. Wass and M. J. E. Sternberg, *Nat. Protoc.*, 2015, 10, 845-858.
5. X. Tan, L. I. Calderon-Villalobos, M. Sharon, C. Zheng, C. V. Robinson, M. Estelle and N. Zheng, *Nature*, 2007, 446, 640-645.